J Fail. Anal. and Preven. (2016) 16:264–270
DOI 10.1007/s11668-016-0077-2

TECHNICAL ARTICLE—PEER-REVIEWED

Fracture Surface Morphology of Delamination Failure of Polymer Fiber Composites Under Different Failure Modes

Pasa Yayla

Submitted: 22 October 2015 / in revised form: 31 December 2015 / Published online: 11 February 2016

Abstract The delamination of fiber reinforced polymer composites is one of the most common failures encountered in industrial applications. The most unique macroscopic and microscopic fracture surface features of the delaminations under different failure modes are of interests not only for practical failure analysis investigations but also it helps to reveal the physics behind the delamination phenomenon. In this work, fracture surface morphology of the delaminated carbon fiber polymer composites under mode I, mode II, and mixed-mode I/II loading conditions is investigated mainly with scanning electron microscopy. The unique fractographic features are identified and discussed. The results on ductile and brittle matrix composites have shown their own features, and most important of all the alignment angle of fibrils in the resin-rich ductile matrix could be correlated with the delamination mode.

Keywords Delamination · Fiber composites · Fractograph · Failure modes

Introduction

Post-mortem investigation of damaged or fractured components at macroscopic as well as microscopic levels could be one of the most effective ways of studying the type and magnitude of applied stress state to the structure and the response of the structure to it. Moreover, the microscopic failure investigation of the broken specimen could be used to verify the failure mechanism and compare different composite systems.

The fracture surface morphology of delaminated fiber reinforced composite materials has been investigated by many researchers. Friedrich [1] investigated the failure mechanisms of delamination in epoxy and poly-ether-ether-ketone (PEEK) composites. He concluded that the principal mechanisms of energy absorption in the composites could be categorized as: (i) fiber bridging, (ii) fiber fracture, (iii) formation of the main fracture surface, (iv) formation of side cracks, and (v) plastic deformation and microcracking of the matrix around the fibers. Johannesson and his co-workers [2] studied fractograph of delaminated graphite/epoxy laminates. Purslow [3, 4] studied the general fractographic features of delamination under peel (mode I) and shear (mode II) failures, respectively. Greenhalgh [5], and Bascom and Gweon [6] detailed delamination micro-mechanisms and matrix fracture morphologies of polymer composites.

The aim of the present study is to investigate the fracture surface of carbon fiber reinforced polymer composites which fractured in different failure modes and analyze the microscopic features in order to understand the mechanism of delamination. Moreover, special attention is given as to whether the failure mode can be predicted from the fracture surface morphology.

Experimental Procedure

The materials used in this study are two different carbon fiber reinforced polymer composites. These are thermoset-based carbon/epoxy composite having a trade name of "Fibredux 6376" and thermoplastic based APC-2, and a tougher polymer composite made of AS4 fibers in poly-

P. Yayla (✉)
Mechanical Engineering Department, Engineering Faculty, Marmara University, Goztepe Campus, 34722 Istanbul, Turkey
e-mail: pasa.yayla@marmara.edu.tr; pyayla@gmail.com

ether-ether-ketone (PEEK) matrix. The former material is supplied by Ciba Geigy in the form of prepreg sheet having continuous unidirectional T-300 carbon fibers supplied by Toray Inc., Japan. The APC-2 system is supplied by Imperial Chemical Industries (ICI), of the UK, and utilizes unidirectional AS4 carbon fibers produced by Herculus Inc., USA. Each material had a fiber volume fraction of about 61%.

The nominal thickness of the panel for most of the specimen is 3.2 mm and made out of 24 plies using the curing procedure recommended by the prepreg manufacturers. However, for fixed ratio mixed-mode tests, the specimens made from 32 plies are used. In order to provide initial delamination, a double layer aluminum foil with a total thickness of 20 μm and a length of 25 mm is inserted at the panel along one edge prior to processing.

In all the experiments, straight-sided double cantilever beam (DCB)-type specimens having a width of approximately 24 mm and length of 145 mm are cut from the composite panels along the fiber direction. Aluminum blocks are bonded to the pre-cracked end of the specimens using the procedure outlined in [7] in order to apply the load perpendicular to the interlaminar layer. The edge of the specimens is painted with a white correction liquid and marked at a 5-mm interval as a means of crack length recording.

The tests are carried out with an Instron 1186 machine at a crosshead velocity of 2 mm/min at room temperature (23 °C). DCB specimens are used for mode I fracture tests. For mode II and mixed-mode (with a ratio of 1.33) tests, one-armed end loaded split (ELS) experiments are performed. For a failure mode of $G_I/G_{II} = 0.5$, a mixed-mode bending test, detailed in Kinloch et al. [8], is utilized.

The broken fracture surfaces are cut from the specimens tested under mode I, mode II, and mixed-mode conditions using a diamond wheel cutter. In order to remove the debris that might be produced during the crack propagation from the surfaces, all the samples are ultrasonically cleaned. After the specimens are vacuum-sputter-coated with gold, the examination is carried out using a Joel JSM 5300 scanning electron microscope (SEM). Tilting the specimen about 25° from its normal position, as in Fig. 1, results in better image characteristics, which might be useful in predicting the failure mode. Therefore, all the specimens are tilted to that angle during the SEM examination.

Results and Discussion

The nature of fracture surfaces could be, in general, divided into four different groups. These are (i) resin fracture, (ii) fiber fracture, (iii) exposed fiber surfaces, and (iv) imprints of resin on the fiber surfaces. From the present

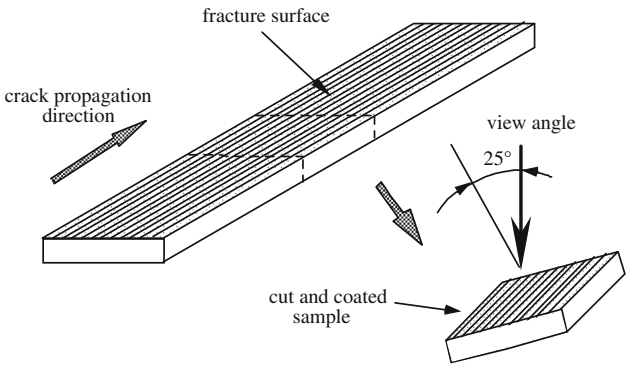

Fig. 1 Schematic representation of the SEM specimen preparation

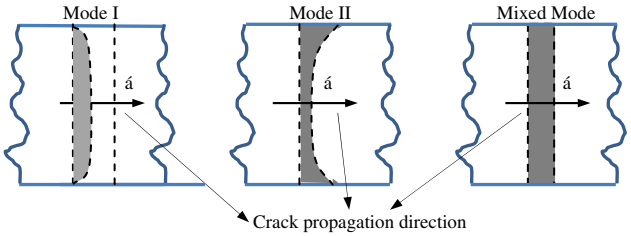

Fig. 2 Delamination crack front shape in different failure modes

investigation, it became clear that the number of fiber fractures in mode I failure is higher than that seen in mode II failure.

The crack front shape of delamination differs from each other in different failure modes. As shown in Fig. 2, the crack front shape is parabolic in mode I, in mode II the crack front leads at sample sides, and in mixed-mode crack front is more or less straight. This variation of the crack front with respect to delamination mode is attributed to the Poisson effects of the beam under bending deformations.

Mode I

SEM microscopic examination of the mode I delamination fracture surfaces reveals that the failures are primarily in the matrix material. As a result, it is mainly the fracture resistance of the matrix material which determines the delamination resistance of the composite. Additionally, the fiber fracture and fiber bridging taking place during the failure process, which are attributed to the material lay-up by Johnson and Mangalgiri [9], are expected to contribute to the delamination resistance.

The mode I delamination fracture surfaces show a number of distinctive features for each material. For epoxy composite, the fracture process takes place in the matrix and leaves a relatively smooth and brittle surface with little fiber exposure, as seen in Fig. 3. There is no significant indication of any extensive plastic deformation in the matrix, or debonding between the matrix and the fibers.

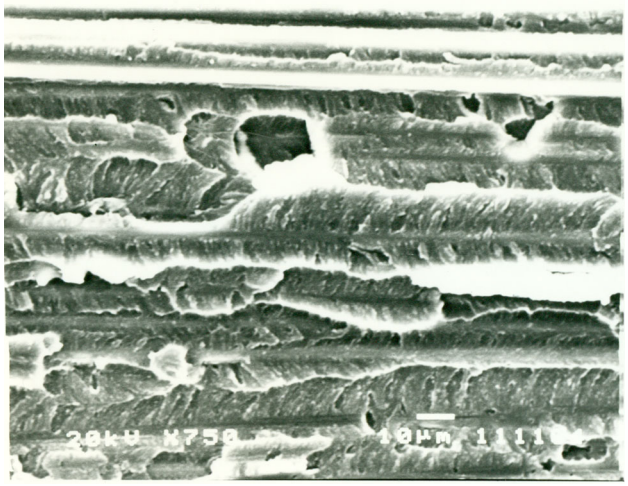

Fig. 3 Mode I fracture surface of epoxy composite

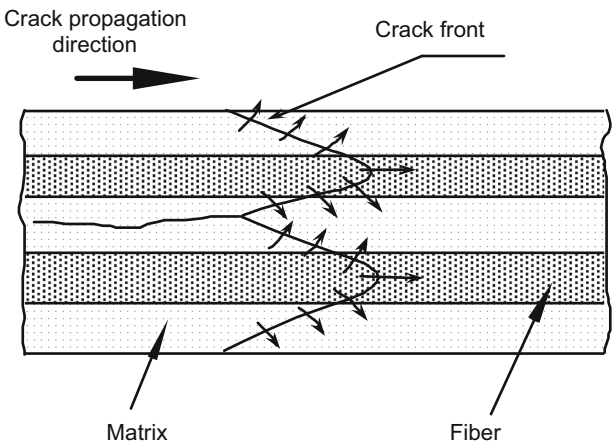

Fig. 4 Sketch of crack front shape in brittle epoxy composite under Mode I

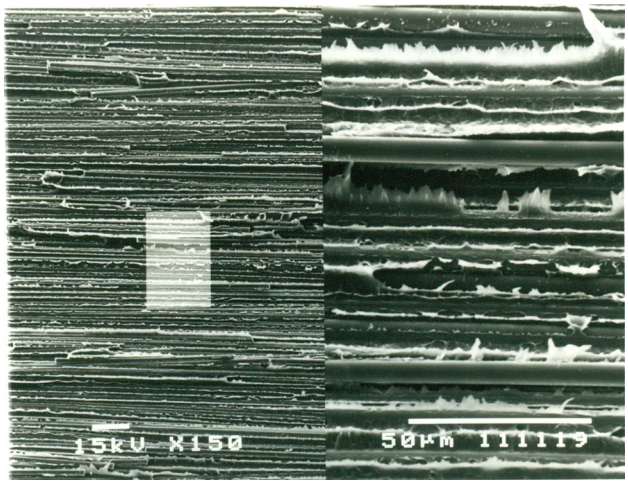

Fig. 5 Mode I fracture surface of PEEK composite

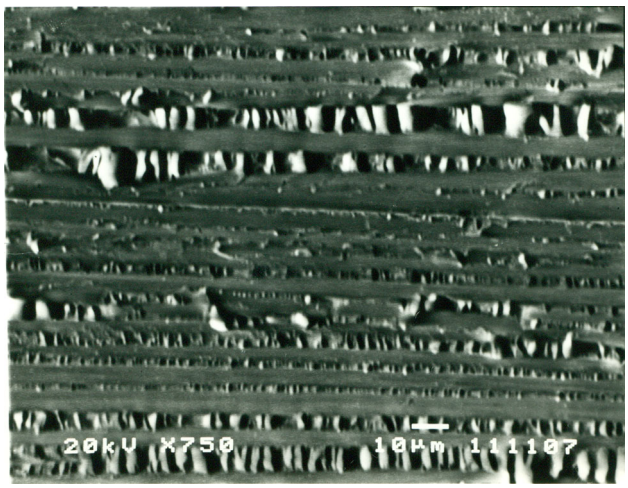

Fig. 6 Mode II fracture surface of epoxy composite

The direction of the crack propagation could be predicted as follows. There are ">" type river marks on the resin surfaces covering the fibers around the "resin-rich" regions on the fiber surface along the fiber axis, the front ends of ">" markings showing the crack propagation direction. These "river lines" between the fibers suggest that the crack front is leading on the fiber mid-surface and proceeds sideways, as shown schematically in Fig. 4. This might be because of the fact that compared to the matrix material, the fiber possesses higher modulus. As a result, the stress intensity factor varies significantly along the crack front, attaining its maximum at the top of individual fibers aligned in the fracture plane. However, for the "resin poor" regions, there are no visible marks indicating the direction (Fig. 3).

One of the main features of the delamination of the PEEK composites is the fact that the crack propagation is not stable but propagates in stick–slip mode. The mode I surface features of PEEK composite are presented in Fig. 5. A closer inspection of the picture shows a remarkably ductile matrix failure around the resin-rich zones and comparatively clear fiber surfaces around the resin-poor areas. The tips of the plastically deformed matrix stand perpendicularly to the fracture surface. With these features, it is not possible to predict the direction of the crack propagation for this composite tested in mode I. The plastic deformation of the matrix taking place between fibers in general with a loose fiber at the middle dominate the fracture surface, suggesting that, as expected, for the PEEK composite the process zone at the crack tip is higher than that in epoxy composite.

Mode II

The main features observed in the mode II fracture surfaces are the relatively clean and exposed fibers with small resin

imprints on them and oriented fractured resin regions between the fibers. This observation suggests that the failure occurs at the interfacial bond, between the fiber and matrix phase. However, the mode II fracture surfaces of the epoxy and PEEK composites differ from each other in many respects. For the former one, the failure of the resin material in between debonded fibers possesses a number of unique features and patterns known as *hackles, serrations* (Johannesson et al. [2]) or *shear cusps* (Friedrich [1]), as shown in Fig. 6. These regular stacking of plates like sheer cusps are perpendicular to the main fracture surface, showing no distinctive crack propagation direction. Johannesson and Blikstad [9] have observed similar marking on angle-ply laminates subjected to peel loading. Johannesson et al. [2] emphasizes that these features are the result of microcracking perpendicular to the principle tensile stress in the matrix between the fibers. From a close examination of the SEM micrographs, it seems that for this type of brittle matrix, a number of micro-cracks are formed at the crack tip perpendicular to the fiber direction by the sheer stresses. Because of the difference in elastic modulus between the fibers and matrix, it appears that these micro-cracks originate on the surface of fibers and are propagated into the matrix by the maximum principle tensile stress. The schematic mechanism of the mode II type delamination in epoxy composites is depicted in Fig. 7. From Figs. 6 and 7, it could be provoked that in mode II type delaminations, the crack tends to propagates in mode I within the matrix-reach region between the fibers.

On PEEK composite mode II fracture surface, Fig. 8, the matrix has undergone extensive plastic deformation, and the tilt direction of this plastically drawn matrix, named "fibril," is roughly that of the maximum shear stress. The mode II delamination failure gives cleaner fiber surfaces in both epoxy and PEEK composites that were studied.

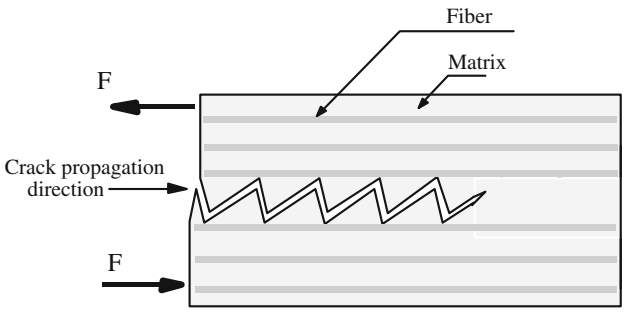

Fig. 7 Sketch of crack propagation mechanism in brittle epoxy composite under Mode II

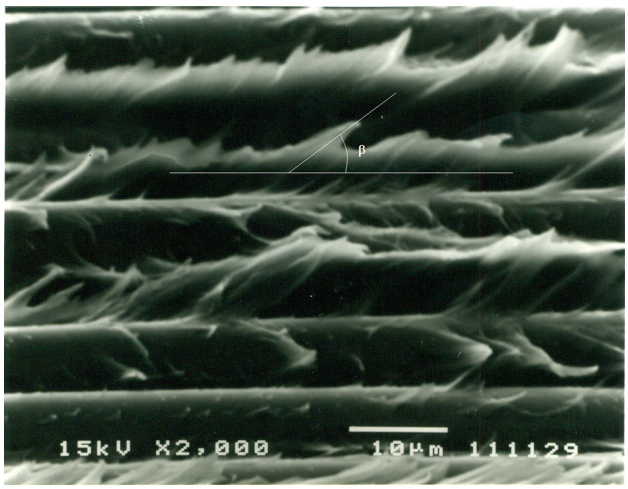

Fig. 9 Fracture surface of PEEK composite failed under mixed-mode ratio of $G_I/G_{II} = 0.5$

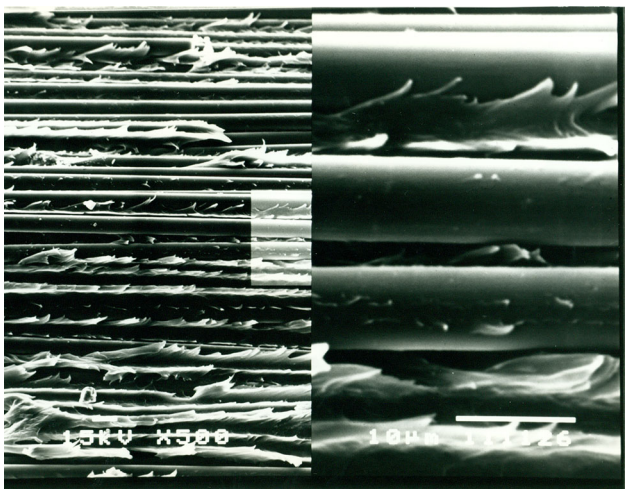

Fig. 8 Mode II fracture surface of PEEK composite

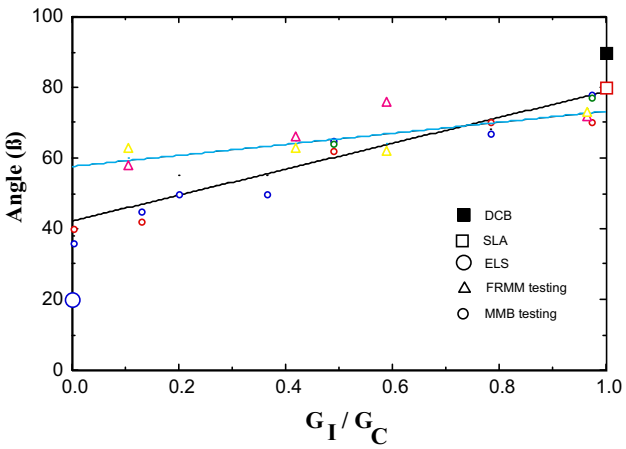

Fig. 10 Variation of fiber alignment with respect to G_I/G_C ratio for PEEK composites for different failure modes

Mixed-Mode Features

In addition to the pure mode I and mode II fracture fractographic analysis, a similar examination is conducted on the two composites tested at G_{IC}/G_{IIC} ratios of 0.5 and 1.33. Depending upon the mixed-mode ratio, the fracture surfaces have their own distinctive features and differ from the pure mode cases in many respects. The characteristic differentiating feature of the surfaces is the tilt direction of the markings along which the fibrils are stretched on the surfaces. The micrographs of PEEK composite tested at G_I/G_{II} ratio of 0.5 is given Fig. 9. A careful examination of the alignment of the deformed matrix material with respect to the fiber axis shows that plastically deformed fibrils direction varies with the mode of loading. The angle between the plastically stretched matrix and fiber, β, varies systematically with mode of loading, as shown in Fig. 10. Figure also indicates some difference between the fixed ratio mixed-mode (FRMM) and mixed-mode bending (MMB) [8] test methods.

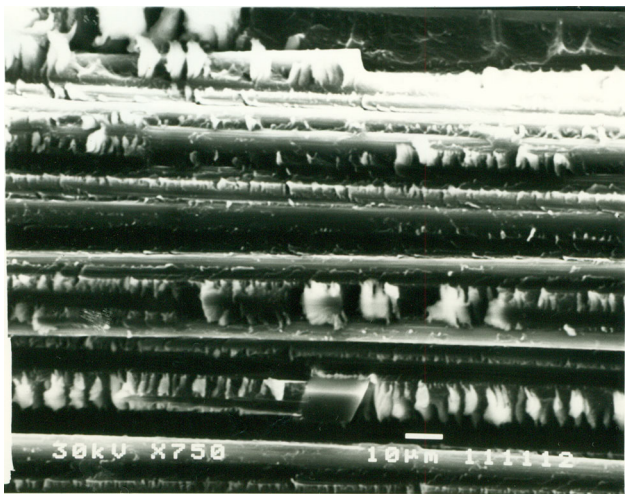

Fig. 11 Fracture surface of epoxy composite failed under mixed-mode ratio of $G_I/G_{II} = 0.5$

The mixed-mode failure of epoxy composite shows the general trend that as the failure mode is shifted from mode I to mode II, the tilt angles of the platelets tend to increase, as seen in Fig. 11. However, identifying this angle for different modes of failure is not an easy task in that although for pure mode II failure the plate seems to be straight, as the failure mode approaches mode I, as pointed out by Johannesson and Blikstad [10], the tips of the plate like features on the surface are deformed along the fiber direction due to the relative motion of the surfaces during crack extension.

A series of SEM examinations was carried out on both epoxy and PEEK composites tested under asymmetric DCB and single-arm loaded (SAL) test modes. The purpose of this examination is to check the existence, and, if possible, predict the amount of the mode II component in these tests.

The difference in the beam thickness in the asymmetric DCB experiments results in different deformation in the each beam, leading to a difference in moment arm length [11]. As the specimen is loaded, the section of the specimen ahead of the crack tip rotated with respect to its initial horizontal direction, and this rotation increased with increasing crack length. For this particular geometry, the rotation in the asymmetric DCB experiments is found to be as high as 10°. The measured fiber alignment angle is found to be about 85°. For the SAL, a closer examination of the SEM surfaces indicated that the plastically stretched matrix fibrils were angled at about 80° with respect to the fiber axis. From the examination of the surfaces, it is seen that the mode II component of the failure tends to be slightly higher in these tests compared to those in asymmetric DCB tests.

Stick–Slip Delamination in Mode I for PEEK Composite

The unstable crack propagation in all modes of delamination occurs in PEEK composite, and this can be easily seen

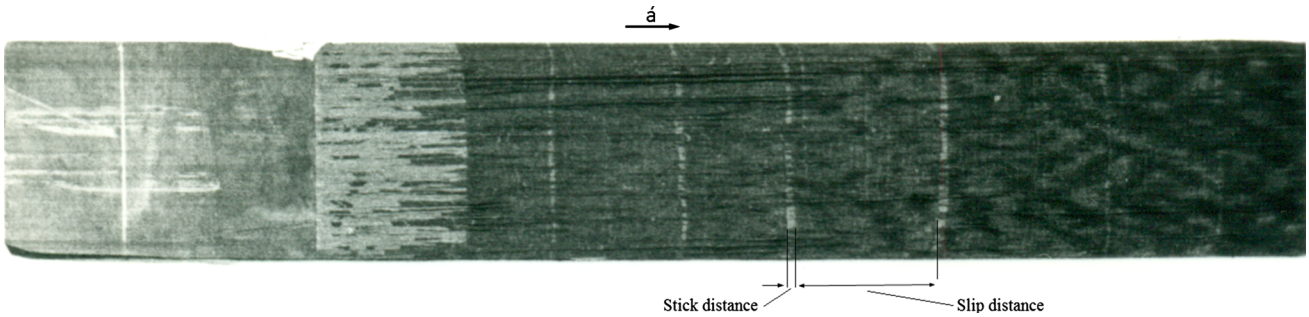

Fig. 12 Stick–slip type delamination in Mode I crack extension in PEEK composite

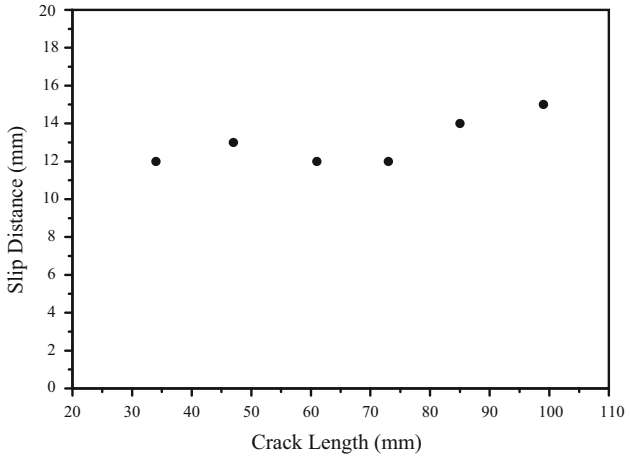

Fig. 13 Variation of slip distance as a function of the crack length in PEEK composite delaminated in Mod I for ram velocity of 0.5 m/s

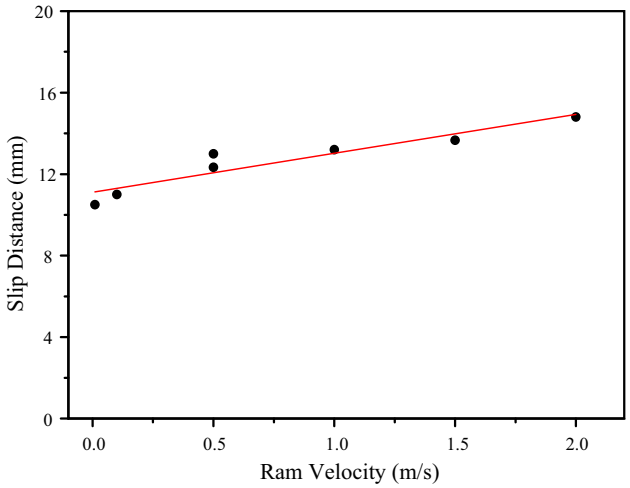

Fig. 14 Variation of slip distance as a function of ram velocity in PEEK composite delaminated in Mod I

on the fracture surfaces revealing itself with changes in crack velocity or even partial arrest of the crack front [5], Fig. 12. The stick–slip delamination growth takes place during the stable and unstable crack growth. The dark and light band regions on the surface are unstable and stable crack growth regimes in delamination, respectively. In the dark regions, there is a relatively little plastic deformation of the matrix compared with the light regions having relatively high plastic deformations. The slip distance in mode I delamination remains fairly constant along the crack length as depicted in Fig. 13. However, this slip distance increase slightly with the ram velocity under mode I delamination, Fig. 14. Although the mechanism of stick–slip delamination is not well understood yet, as pointed out by Yayla and Leevers [12], it could be envisaged that for the crack propagation in ductile polymers at a given temperature, there is a minimum steady state crack velocity below which crack propagation cannot be sustained. Thus a crack can only propagate if the crack driving force is high enough to force the crack to propagate above this minimum crack speed threshold limit.

Discussion and Conclusions

This study is committed to the subject of fracture surface features of delamination of fiber composites under different failure modes. The study, for the first time, presents unified failure mechanisms under pure mode I, mode II, and mixed-mode I/II under quasi-static and dynamic loadings and highlights the characteristic features, differentiating the failure mode. The interlaminar delamination behavior in modes I, II, and mixed-mode of I/II have been studied for two composites with the same AS4 carbon fiber and two different matrix types, namely epoxy and PEEK. The SEM photographic features of delamination of fiber reinforced composites fractured under different modes are identified. The morphology of the surfaces could be divided into two main categorizes: ‘resin-rich’ and ‘resin-poor’ regions. Moreover, the surface features reflect different distinctions for different failure modes. Mode II failure shows an abundance of exposed fibers partly embedded in the resin. However, in mode I case, the surfaces are covered with resin and some fiber imprints are visible. The alignment angle of the stretched fibrils on the fracture surfaces indicated that for pure mode I case the fibrils are vertically aligned, i.e., 90°, to the surfaces, but a small amount of mode II component significantly reduces the angle, which results in an increase in the strain energy release rate, G_C. Similarly, the minimum alignment angle of about 20°, thus the maximum G_C, is attained in pure mode II type loading and a small amount of mode I failure mode increased that alignment angle quite remarkably, indicating lower G_C. For the asymmetric DCB and SAL specimens, the fracture surface morphology obtained from SEM examination together with the fracture energy calculations suggest that the local analysis used in data reduction in calculating G_C gives better results over the global analysis. For the FRMM tests, whoever, the global method of analysis predicts better values which are in good agreement with those obtained from other test methods.

Acknowledgments The author wishes to acknowledge the support of Mechanical Engineering Department—Imperial College of Science, Technology and Medicine (UK) throughout a project; in particular, James Gordon Williams, Anthony James Kinloch, and Bamber Blackman for their contribution.

References

1. K. Friedrich, Fractographic analysis of polymer composites, in *Application of Fracture Mechanics to Composite Materials*, ed. by K. Friedrich (Elsevier, Amsterdam, 1989)
2. T. Johannesson, R. Sjöblom, R. Seldén, The detailed structure of delamination fracture surfaces in graphite/epoxy laminates. J. Mater. Sci. **19**, 1171–1177 (1984)
3. D. Purslow, Matrix fractography of fibre-reinforced thermoplastics, Part 1. Peel failures. Composites **18**(5), 365–374 (1987)
4. D. Purslow, Matrix fractography of fibre-reinforced thermoplastics, Part 2. Shear failures. Composites **19**(2), 115–126 (1988)
5. E.S. Greenhalgh, *Failure Analysis and Fractography of Polymer Composites* (Woodhead Publishing Ltd., Cambridge, 2009)
6. W.D. Bascom, S.Y. Gweon, Fractography and failure mechanisms of carbon fibre-reinforced composite materials, in *Fractography and Failure Mechanisms of Polymer and Composites*, ed. by A.C. Roulin-Moloney (Elsevier, London, 1989)
7. S. Hashemi, A.J. Kinloch, J.G. Williams, The analysis of interlaminar fracture in uniaxial fibre-polymer composites. Proc. R. Soc. Lond. A **427**, 173–199 (1990)
8. A.J. Kinloch, Y. Wang, J.G. Williams, P. Yayla, An experimental analysis of mixed-mode delamination tests for composite materials. Compos. Sci. Technol. **47**, 226–237 (1992)
9. W.S. Johnson, P.D. Mangalgiri, *Investigating of Fibre Bridging in Double Cantilever Beam Specimens*, NASA Technical Memorandum 87716 (NASA, Hampton, 1986)
10. T. Johannesson, M. Blikstad, Fractography and fracture criteria of the delamination process, in *Delamination and Debonding of Materials*, ASTM STP 876, ed. by W.S. Johnson (American Society for Testing and Materials, Philadelphia, 1985), pp. 411–423
11. M. Charalambides, A.J. Kinloch, Y. Wang, J.G. Williams, On the analysis of mixed-mode failure. Int. J. Fract. **54**, 269–291 (1992)
12. P. Yayla, P.S. Leevers, Rapid crack propagation in pressurised plastic pipe—II Critical pressures for polyethylene pipe. Eng. Fract. Mech. **42**(4), 675–682 (1992)